



# Impacts of the hygro-thermo conditions on the vibration analysis of 2D-FG nanoplates based on a novel HSDT

Zhenya Zhang<sup>1,2</sup> · Xiaoli Liu<sup>2</sup> · Reza Mohammadi<sup>3</sup>

Received: 4 March 2021 / Accepted: 4 June 2021 / Published online: 15 June 2021

© The Author(s), under exclusive licence to Springer-Verlag London Ltd., part of Springer Nature 2021, corrected publication 2021

## Abstract

The main purpose of this paper is to render a novel higher-order shear deformation theory (HSDT), which can model the dynamic analysis of the 2D-FG nanoplates subjected to hygro-thermo loading using a new shear strain shape function. The transverse component of displacement is composed of bending and shear parts. Thickness stretching influence is considered according to higher-order shear and normal deformation theory. The present model is suitable to deal with thin and thick nanoplates since it includes the HSDT and the thickness stretching influence. Assume the plate's materials properties, including density, Young's modulus, and thermal and moisture parameters vary continuously with an arbitrary function in two directions. Size-dependent nonlocal elasticity theory is dedicated to consider the nonlocality. The temperature variation and moisture expansion vary through the thickness of the nanoplate nonlinearly. To achieve the equations of motion of the 2D-FG nanoplate with simply-supported boundary conditions, Hamilton's principle is utilized. Navier method is utilized for a closed-form solution of the 2D-FG nanoplates. The impacts of several parameters, including thermal effects, are investigated on the vibration characteristics of the 2D-FG nanoplates. The results demonstrate that with increasing the FG indexes, their impacts on the natural frequency of the system will enhance/reduce when the temperature variation increases/reduces.

**Keywords** 2D-FG plates · Novel HSDT · Small scale effect · Thickness stretching · Hygro-thermo-environment

## 1 Introduction

Functionally graded materials (FGMs) are the new kinds of composites that are made from a composition from ceramics and metals. These kinds of heterogeneous materials have variable mechanical properties in one or more directions. The usages of FGMs have been enhanced quickly in all of the engineering branches, such as mechanical engineering, due to their phenomenal mechanical properties. Therefore, to have a comprehensive investigation about their features, many researchers examined the mechanical responses of the FGMs with variable mechanical properties in one or more directions [1–12].

Kazemirad et. al [13] examined the nonlinear dynamic investigation of a buckled axially moving beam. Ghayesh et. al [14] examined the vibration investigation of a simply supported spring-mass-beam system considering the thermal efficacy. Ghayesh et. al [15] presented an approximate analytical solution technique for phase-shift prediction along the length of the measuring tube of a Coriolis mass-flowmeter. Ghayesh and Amabili [16] examined the nonlinear stability of an axially moving beam in the thermal environment. Daikh et. al [17] examined the vibration investigation of the FG sandwich nanoplates in the thermal environment based on third-order shear deformation theory (TSDT). Nonlocal elasticity theory is utilized to consider nonlocality. Hosseini et. al [18] studied the free vibration investigation of the nanoplates subjected to thermal efficacy using FSDT. To ponder the thermal efficacy, linear thermal relation is utilized. Daikh et. al [19] examined the buckling and free vibration investigation of the reinforced composite nanoplates reinforced by carbon nanotubes in the thermal environment based on TSDT. Nonlocal strain gradient theory is utilized to ponder the nonlocality. Singh and Azam [20] examined the buckling and free vibration investigation of

✉ Xiaoli Liu  
L13600620263@sina.com

<sup>1</sup> School of Architecture and Transportation Engineering, Ningbo University of Technology, Ningbo 315211, China

<sup>2</sup> State Key Laboratory of Hydroscience and Engineering, Tsinghua University, Beijing 100084, China

<sup>3</sup> Department of Mechanical Engineering, Tarbiat Modares University, Tehran, Iran

the FG nanoplates in the thermal environment based on non-local elasticity theory. Dastjerdi et. al [21] examined the bending investigation of the thick porous FG nanoplates in a hygro-thermal environment based on nonlocal elasticity theory. Chen et. al [22] studied the vibration examination of the nanoplates subjected to thermal loading based on fourth-order strain gradient theory. Fang et. al [23] examined the buckling investigation of the FG composite skew nanoplates with various boundary conditions. Kolahdouzan et. al [24] studied the vibration and buckling investigation of the FG-CNTRC sandwich annular nanoplates based on nonlocal elasticity theory. Dindarloo and Zenkour [25] studied the bending responses of the FG spherical nanoshells in the thermal environment. Linear relations are utilized to ponder the thermal efficacy based on nonlocal strain gradient theory. Mashat et. al [26] examined the bending responses of the FG plates under the hygro-thermo-mechanical loading based on a quasi-3D higher-order plate theory. Lal and Saini [27] examined the vibration investigation of the FG circular plates with nonlinear temperature distribution in the thickness direction. Thang et. al [28] examined the free vibration investigation of the FG nanoplates reinforced with carbon nanotubes based on nonlocal strain gradient theory. Arshid et. al [29] studied the free vibration and buckling investigation of the FG porous sandwich curved microbeams in the thermal environment based on modified couple stress theory. Esen et. al [30] examined the vibrational behavior of the FG cracked microbeam rested on an elastic foundation subjected to the thermal and magnetic fields.

Pursuant to the above review, the free vibration investigation of the 2D-FG nanoplate subjected to hygro-thermo loading based on a novel HSDT is examined for the first time. The size-dependent nonlocal higher-order theory is dedicated to pondering the nonlocality. The novelty of the current research is to present a new HSDT, which is an amalgamation of exponential, polynomial and trigonometric functions. Thickness stretching influence is considered according to higher-order shear and normal deformation theory. The transverse component of displacement is composed of bending and shear parts. We ponder the nonlinear relations for temperature and moisture fields to investigate the impacts of the thermal and moisture efficacy on the vibration characteristics of the 2D-FG nanoplates. Hamilton’s axiom is dedicated to achieving the governing equations of motion. Then, Navier solution technique is dedicated to deriving the natural frequency of the nanoplates with S–S boundary conditions. The effects of the various parameters are examined on the vibration characteristics of the 2D-FG nanoplates.

## 2 Size-dependent analysis of the 2D-FG nanoplates

In the current research, we use the two-directional (2D) functionally graded materials (FGMs) to investigate the vibration characteristics of the nanoplates subjected to hygro-thermo conditions. Assume the materials’ properties of the plate including density ( $\rho$ ), Young’s modulus ( $E$ ) and thermal and moisture parameters vary continuously with an arbitrary function in two directions as below.

$$\begin{aligned}
 E(x, z) &= e^{\frac{n_1 x}{a}} \left[ E_c \left( \frac{2z+h}{2h} \right)^{n_2} + E_m \left( \frac{2z+h}{2h} \right)^{n_2} \right] \\
 \rho(x, z) &= e^{\frac{m_1 x}{a}} \left[ \rho_c \left( \frac{2z+h}{2h} \right)^{m_2} + \rho_m \left( \frac{2z+h}{2h} \right)^{m_2} \right] \\
 \alpha(x, z) &= e^{\frac{n_3 x}{a}} \left[ \alpha_c \left( \frac{2z+h}{2h} \right)^{n_4} + \alpha_m \left( \frac{2z+h}{2h} \right)^{n_4} \right] \\
 \beta(x, z) &= e^{\frac{m_3 x}{a}} \left[ \beta_c \left( \frac{2z+h}{2h} \right)^{m_4} + \beta_m \left( \frac{2z+h}{2h} \right)^{m_4} \right],
 \end{aligned} \tag{1}$$

where  $n_i, m_j (i, j = 1, \dots, 4)$  are the FG indexes;  $\alpha$  and  $\beta$  are the thermal and moisture parameters, respectively. In the current research, we consider a rectangular nanoplate with length  $a$ , width  $b$  and thickness  $h$  (Fig. 1). In the present model, thickness stretching influence is considered according to higher-order shear and normal deformation theory. To study the vibration characteristics of the 2D-FG nanoplates based on a new HSDT, the displacement field is reported as below [31]:

$$\begin{aligned}
 u_x(x, y, z, t) &= u(x, y, t) - z \frac{\partial w_b(x, y, t)}{\partial x} - f(z) \frac{\partial w_s(x, y, t)}{\partial x} \\
 u_y(x, y, z, t) &= v(x, y, t) - z \frac{\partial w_b(x, y, t)}{\partial y} - f(z) \frac{\partial w_s(x, y, t)}{\partial y} \\
 u_z(x, y, z, t) &= w_b(x, y, t) + w_s(x, y, t) + g(z)w_z(x, y, t),
 \end{aligned} \tag{2}$$

where  $u_x, u_y$  and  $u_z$  are three parts of the displacement along with the  $x, y$  and  $z$  directions, respectively; The transverse deflection is divided to shear ( $w_s$ ) and bending ( $w_b$ ) parts;  $w_z$  is the thickness stretching parameter.

The main novelty of the present research is to render a new HSDT without including the shear correction coefficient. The new shear strain shape function  $f(z)$  presented in this research is an amalgamation of exponential, polynomial and trigonometric functions. According to this HSDT, we can investigate the mechanical responses of the composite structures, including FG plates and shells, accurately. To compare the present theory with the other theories, the variations of  $f(z)$  and  $\frac{df(z)}{dz}$  is presented along with the thickness direction in Fig. 2.

$$f(z) = h \tan^{-1} \left( \frac{z}{h} \right) + \frac{4z^3}{15h^2} + \frac{h}{\pi} \sin \left( \frac{\pi z}{h} \right) - z. \tag{3}$$

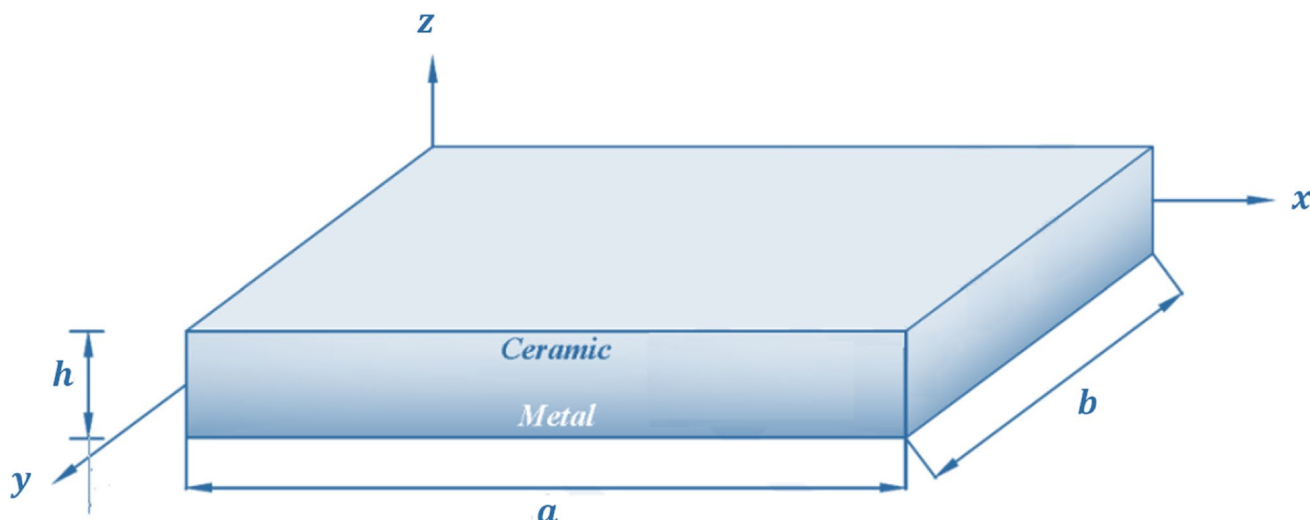


Fig. 1 Geometry of a rectangular FG nanoplate

With considering the displacement field, the strain parts are reported as:

$$\begin{aligned}
 \epsilon_1 &= \frac{\partial u_x}{\partial x} = \frac{\partial u}{\partial x} - z \frac{\partial^2 w_b}{\partial x^2} - f(z) \frac{\partial^2 w_s}{\partial x^2} \\
 \epsilon_2 &= \frac{\partial u_y}{\partial y} = \frac{\partial v}{\partial y} - z \frac{\partial^2 w_b}{\partial y^2} - f(z) \frac{\partial^2 w_s}{\partial y^2} \\
 \epsilon_3 &= \frac{\partial u_z}{\partial z} = \frac{dg}{dz} w_z \\
 \epsilon_6 &= \frac{\partial u_x}{\partial y} + \frac{\partial u_y}{\partial x} = \frac{\partial u}{\partial y} + \frac{\partial v}{\partial x} - 2z \frac{\partial^2 w_b}{\partial x \partial y} - 2f(z) \frac{\partial^2 w_s}{\partial x \partial y} \\
 \epsilon_4 &= \frac{\partial u_x}{\partial z} + \frac{\partial u_z}{\partial x} = \left(1 - \frac{df}{dz}\right) \frac{\partial w_s}{\partial x} + g(z) \frac{\partial w_z}{\partial x} \\
 \epsilon_5 &= \frac{\partial u_y}{\partial z} + \frac{\partial u_z}{\partial y} = \left(1 - \frac{df}{dz}\right) \frac{\partial w_s}{\partial y} + g(z) \frac{\partial w_z}{\partial y}.
 \end{aligned} \tag{4}$$

In this paper, to ponder the nonlocality, the size-dependent nonlocal elasticity theory is dedicated. The relations between the stress and strain components with considering the thermal and moisture impacts are:

$$(1 - \mu^2 \nabla^2) \begin{Bmatrix} \sigma_1 \\ \sigma_2 \\ \sigma_3 \\ \sigma_6 \\ \sigma_4 \\ \sigma_5 \end{Bmatrix} = \begin{bmatrix} C_{11} & C_{12} & C_{13} & 0 & 0 & 0 \\ C_{12} & C_{22} & C_{23} & 0 & 0 & 0 \\ C_{13} & C_{23} & C_{33} & 0 & 0 & 0 \\ 0 & 0 & 0 & C_{66} & 0 & 0 \\ 0 & 0 & 0 & 0 & C_{44} & 0 \\ 0 & 0 & 0 & 0 & 0 & C_{55} \end{bmatrix} \begin{Bmatrix} \epsilon_1 - \alpha_{11} \Delta T - \beta_{11} \Delta C \\ \epsilon_2 - \alpha_{22} \Delta T - \beta_{33} \Delta C \\ \epsilon_3 - \alpha_{22} \Delta T - \beta_{33} \Delta C \\ \epsilon_6 \\ \epsilon_4 \\ \epsilon_5 \end{Bmatrix}, \tag{5}$$

where  $C_{ij}$  are the stiffness parameters:

$$\begin{aligned}
 C_{ii}(x, y, T) &= \frac{E(x, y, T)(1 - \nu)}{(1 + \nu)(1 - 2\nu)}, \quad i = 1, 2, 3 \\
 C_{ii}(x, y, T) &= \frac{E(x, y, T)}{2(1 + \nu)}, \quad i = 4, 5, 6 \\
 C_{12}(x, y, T) &= C_{23}(x, y, T) = C_{13}(x, y, T) = \frac{E(x, y, T)\nu}{(1 + \nu)(1 - 2\nu)}.
 \end{aligned} \tag{6}$$

To study the effects of the thermal and moisture effects on the vibration characteristics of the 2D-FG nanoplates accurately, we ponder the nonlinear relations for temperature and moisture fields as following:

$$\begin{Bmatrix} T(x, y, z) \\ C(x, y, z) \end{Bmatrix} = \begin{Bmatrix} T_1(x, y) \\ C_1(x, y) \end{Bmatrix} + \frac{z}{h} \begin{Bmatrix} T_2(x, y) \\ C_2(x, y) \end{Bmatrix} + \frac{f(z)}{h} \begin{Bmatrix} T_3(x, y) \\ C_3(x, y) \end{Bmatrix}, \tag{7}$$

where  $T_i$  and  $C_i$  are thermal and moisture loads.

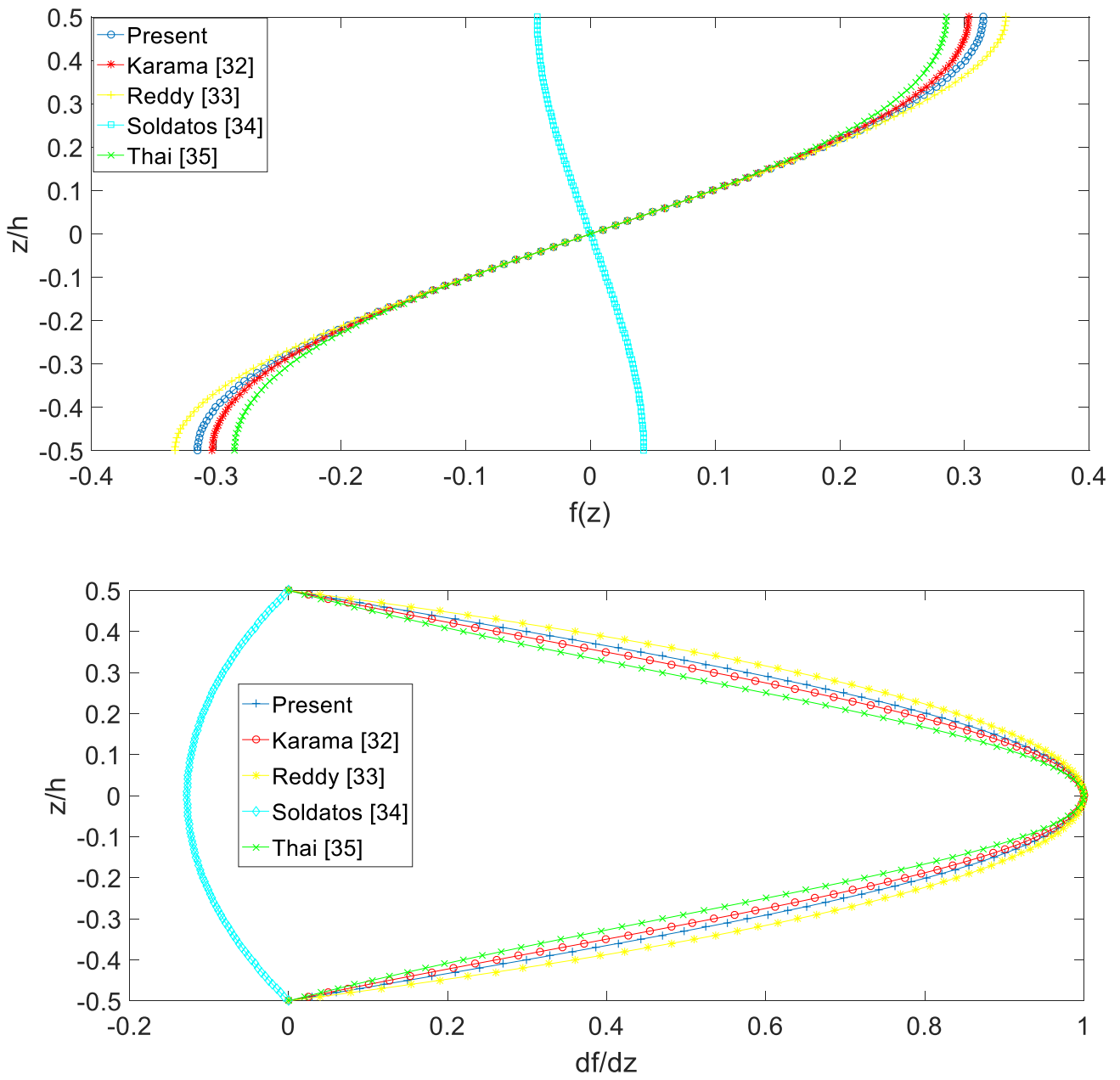


Fig. 2 Variation of  $f(z)$  and  $\frac{df}{dz}$  in several theories

Based on the nonlocal elasticity theory, the stress tensor parts in terms of displacement ingredients with considering the thermal and moisture effects are reported as below:

Implementing Eqs. (2) and (8) into Eq. (9), the governing equation of motion is reported as

$$\begin{aligned}
 (1 - \mu^2 \nabla^2) \sigma_1 &= C_{11} \left( \frac{\partial u}{\partial x} - z \frac{\partial^2 w_b}{\partial x^2} - f(z) \frac{\partial^2 w_s}{\partial x^2} \right) + C_{12} \left( \frac{\partial v}{\partial y} - z \frac{\partial^2 w_b}{\partial y^2} - f(z) \frac{\partial^2 w_s}{\partial y^2} \right) \\
 &\quad + C_{13} \frac{dg}{dz} w_z - C_{11} (\alpha_{11} \Delta T + \beta_{11} \Delta C) - C_{12} (\alpha_{22} \Delta T + \beta_{22} \Delta C) - C_{13} (\alpha_{33} \Delta T + \beta_{33} \Delta C) \\
 (1 - \mu^2 \nabla^2) \sigma_2 &= C_{12} \left( \frac{\partial u}{\partial x} - z \frac{\partial^2 w_b}{\partial x^2} - f(z) \frac{\partial^2 w_s}{\partial x^2} \right) + C_{22} \left( \frac{\partial v}{\partial y} - z \frac{\partial^2 w_b}{\partial y^2} - f(z) \frac{\partial^2 w_s}{\partial y^2} \right) \\
 &\quad + C_{23} \frac{dg}{dz} w_z - C_{12} (\alpha_{11} \Delta T + \beta_{11} \Delta C) - C_{22} (\alpha_{22} \Delta T + \beta_{22} \Delta C) - C_{23} (\alpha_{33} \Delta T + \beta_{33} \Delta C) \\
 (1 - \mu^2 \nabla^2) \sigma_3 &= C_{13} \left( \frac{\partial u}{\partial x} - z \frac{\partial^2 w_b}{\partial x^2} - f(z) \frac{\partial^2 w_s}{\partial x^2} \right) + C_{23} \left( \frac{\partial v}{\partial y} - z \frac{\partial^2 w_b}{\partial y^2} - f(z) \frac{\partial^2 w_s}{\partial y^2} \right) \\
 &\quad + C_{33} \frac{dg}{dz} w_z - C_{13} (\alpha_{11} \Delta T + \beta_{11} \Delta C) - C_{23} (\alpha_{22} \Delta T + \beta_{22} \Delta C) - C_{33} (\alpha_{33} \Delta T + \beta_{33} \Delta C) \\
 (1 - \mu^2 \nabla^2) \sigma_6 &= C_{66} \left( \frac{\partial u}{\partial y} + \frac{\partial v}{\partial x} - 2z \frac{\partial^2 w_b}{\partial x \partial y} - 2f(z) \frac{\partial^2 w_s}{\partial x \partial y} \right) \\
 (1 - \mu^2 \nabla^2) \sigma_4 &= C_{44} \left( \left( 1 - \frac{df}{dz} \right) \frac{\partial w_s}{\partial x} + g(z) \frac{\partial w_z}{\partial x} \right) \\
 (1 - \mu^2 \nabla^2) \sigma_5 &= C_{55} \left( \left( 1 - \frac{df}{dz} \right) \frac{\partial w_s}{\partial y} + g(z) \frac{\partial w_z}{\partial y} \right).
 \end{aligned} \tag{8}$$

Considering the strain potential energy ( $U_S$ ) and kinetic energy ( $U_T$ ) and according to Hamilton’s principle, we have:

$$\begin{aligned}
 &\int_{t_1}^{t_2} (\delta U_T - \delta U_S + \delta U_W) dt \\
 = 0 \Rightarrow &\int_{t_1}^{t_2} \int_0^a \int_0^b \int_{-\frac{h}{2}}^{\frac{h}{2}} (\sigma_1 \delta \varepsilon_1 + \sigma_2 \delta \varepsilon_2 \\
 &+ \sigma_3 \delta \varepsilon_3 + \sigma_4 \delta \varepsilon_4 + \sigma_5 \delta \varepsilon_5 + \sigma_6 \delta \varepsilon_6) dx dy dz dt \\
 &- \int_{t_1}^{t_2} \int_0^a \int_0^b \delta \int_{-\frac{h}{2}}^{\frac{h}{2}} \rho (\dot{u}_x^2 + \dot{u}_y^2 + \dot{u}_z^2) dx dy dz dt = 0.
 \end{aligned} \tag{9}$$

$$\begin{aligned}
 \delta u_x : &\frac{\partial N_1}{\partial x} + \frac{\partial N_6}{\partial y} = -I_3 \frac{\partial \ddot{w}_s}{\partial x} - I_1 \frac{\partial \ddot{w}_b}{\partial x} + I_0 \ddot{u} + q_1 \\
 \delta u_y : &\frac{\partial N_2}{\partial y} + \frac{\partial N_6}{\partial x} = -I_3 \frac{\partial \ddot{w}_s}{\partial y} + I_0 \ddot{v} - I_1 \frac{\partial \ddot{w}_b}{\partial y} + q_2 \\
 \delta w_b : &\frac{\partial^2 M_1}{\partial x^2} + \frac{\partial^2 M_2}{\partial y^2} + 2 \frac{\partial^2 M_6}{\partial x \partial y} = -I_4 \frac{\partial^2 \ddot{w}_s}{\partial y^2} + I_0 (\ddot{w}_b + \ddot{w}_s) + I_6 \ddot{w}_z \\
 &- I_2 \frac{\partial^2 \ddot{w}_b}{\partial x^2} + I_1 \frac{\partial \ddot{u}}{\partial x} + I_1 \frac{\partial \ddot{v}}{\partial y} - I_4 \frac{\partial^2 \ddot{w}_s}{\partial x^2} - I_2 \frac{\partial^2 \ddot{w}_b}{\partial y^2} + q_3 \\
 \delta w_s : &\frac{\partial^2 P_1}{\partial x^2} + \frac{\partial^2 P_2}{\partial y^2} + 2 \frac{\partial^2 P_6}{\partial x \partial y} + \frac{\partial Q_4}{\partial x} + \frac{\partial Q_5}{\partial y} = -I_5 \frac{\partial^2 \ddot{w}_s}{\partial y^2} - I_4 \frac{\partial^2 \ddot{w}_b}{\partial y^2} \\
 &+ I_0 \ddot{w}_b + I_0 \ddot{w}_s - I_4 \frac{\partial^2 \ddot{w}_b}{\partial x^2} + I_3 \frac{\partial \ddot{u}}{\partial x} + I_3 \frac{\partial \ddot{v}}{\partial y} - I_5 \frac{\partial^2 \ddot{w}_s}{\partial x^2} + I_6 \ddot{w}_z + q_4 \\
 \delta w_z : &\frac{\partial Q_4}{\partial x} + \frac{\partial Q_5}{\partial y} - P_3 = I_6 \ddot{w}_b + I_6 \ddot{w}_s + I_7 \ddot{w}_z + q_5.
 \end{aligned} \tag{10}$$

The unknown components of Eq. (10) including the thermal loads and moments due to the hydro-thermo conditions are reported as:

$$\begin{aligned}
(I_0, I_1, I_2, I_3, I_4, I_5, I_6, I_7) &= \int_{-\frac{h_e}{2}}^{\frac{h_e}{2}} \rho(x, y, z) (1, z, z^2, f, fz, fz^2, g, g^2) dz \\
(N_i, M_i, P_i) &= \int_{-\frac{h}{2}}^{\frac{h}{2}} \sigma_i(1, z, f) dz \quad (i = 1, 2, 6) \\
(N_{ii}^T, M_{ii}^T, P_{ii}^T) &= \int_{-\frac{h}{2}}^{\frac{h}{2}} (C_{i1} + C_{i2} + C_{i3})(\alpha\Delta T + \beta\Delta C)(1, z, f) dz \quad (i = 1, 2, 6) \\
(N_{12}^T, M_{12}^T, P_{12}^T) &= \int_{-\frac{h}{2}}^{\frac{h}{2}} (C_{66})(\alpha\Delta T + \beta\Delta C)(1, z, f) dz \\
N_{33}^T &= \int_{-\frac{h}{2}}^{\frac{h}{2}} (C_{13} + C_{23} + C_{33})(\alpha\Delta T + \beta\Delta C) \frac{dg}{dz} dz \\
Q_i &= \int_{-\frac{h}{2}}^{\frac{h}{2}} \sigma_i g dz \quad (i = 4, 5) \\
Q_3 &= \int_{-\frac{h}{2}}^{\frac{h}{2}} \frac{dg}{dz} \sigma_z dz \\
q_1 &= \frac{\partial N_{11}^T}{\partial x} + \frac{\partial N_{12}^T}{\partial y} \\
q_2 &= \frac{\partial N_{12}^T}{\partial x} + \frac{\partial^2 M_{22}^T}{\partial y^2} \\
q_3 &= -q + \frac{\partial^2 M_{11}^T}{\partial x^2} + 2 \frac{\partial^2 M_{12}^T}{\partial x \partial y} + \frac{\partial^2 M_{22}^T}{\partial y^2} \\
q_4 &= -q + \frac{\partial^2 P_{11}^T}{\partial x^2} + 2 \frac{\partial^2 P_{12}^T}{\partial x \partial y} + \frac{\partial^2 P_{22}^T}{\partial y^2} \\
q_5 &= N_{33}^T.
\end{aligned} \tag{11}$$

To achieve the equations of motion in terms of displacement ingredients, it is essential to substitute Eqs. (8) and (11) into Eq. (10) as below:

$$\begin{aligned}
&A_{11} \frac{\partial^2 u}{\partial x^2} - B_{11} \frac{\partial^3 w_b}{\partial x^3} - D_{11} \frac{\partial^3 w_s}{\partial x^3} + A_{12} \frac{\partial^2 v}{\partial x \partial y} - B_{12} \frac{\partial^3 w_b}{\partial x \partial y^2} - D_{12} \frac{\partial^3 w_s}{\partial x \partial y^2} + E'_{13} \frac{\partial w_z}{\partial x} \\
&+ \frac{\partial A_{11}}{\partial x} \frac{\partial u}{\partial x} - \frac{\partial B_{11}}{\partial x} \frac{\partial^2 w_b}{\partial x^2} - \frac{\partial D_{11}}{\partial x} \frac{\partial^2 w_s}{\partial x^2} + \frac{\partial A_{12}}{\partial x} \frac{\partial v}{\partial y} - \frac{\partial B_{12}}{\partial x} \frac{\partial^2 w_b}{\partial y^2} - \frac{\partial D_{12}}{\partial x} \frac{\partial^2 w_s}{\partial y^2} + \frac{\partial E'_{13}}{\partial x} w_z \\
&+ A_{66} \frac{\partial^2 u}{\partial y^2} + A_{66} \frac{\partial^2 v}{\partial x \partial y} - 2B_{66} \frac{\partial^3 w_b}{\partial x \partial y^2} - 2D_{66} \frac{\partial^3 w_s}{\partial x \partial y^2} = (1 - \mu^2 \nabla^2) \left( I_0 \ddot{u} - I_1 \frac{\partial \ddot{w}_b}{\partial x} - I_3 \frac{\partial \ddot{w}_s}{\partial x} + q_1 \right)
\end{aligned} \tag{12a}$$

$$\begin{aligned}
 & A_{12} \frac{\partial^2 u}{\partial x \partial y} - B_{12} \frac{\partial^3 w_b}{\partial x^2 \partial y} - D_{12} \frac{\partial^3 w_s}{\partial x^2 \partial y} + A_{22} \frac{\partial^2 v}{\partial y^2} - B_{22} \frac{\partial^3 w_b}{\partial y^3} - D_{22} \frac{\partial^3 w_s}{\partial y^3} + E'_{23} \frac{\partial w_z}{\partial y} \\
 & + A_{66} \frac{\partial^2 u}{\partial x \partial y} + A_{66} \frac{\partial^2 v}{\partial x^2} - 2B_{66} \frac{\partial^3 w_b}{\partial x^2 \partial y} - 2D_{66} \frac{\partial^3 w_s}{\partial x^2 \partial y} + \frac{\partial A_{66}}{\partial x} \frac{\partial u}{\partial y} + \frac{\partial A_{66}}{\partial x} \frac{\partial v}{\partial x} - 2 \frac{\partial B_{66}}{\partial x} \frac{\partial^2 w_b}{\partial x \partial y} - 2 \frac{\partial D_{66}}{\partial x} \frac{\partial^2 w_s}{\partial x \partial y} \\
 & = (1 - \mu^2 \nabla^2) \left( I_0 \ddot{v} - I_1 \frac{\partial \ddot{w}_b}{\partial y} - I_3 \frac{\partial \ddot{w}_s}{\partial y} + q_2 \right)
 \end{aligned} \tag{12b}$$

$$\begin{aligned}
 & B_{11} \frac{\partial^3 u}{\partial x^3} - E_{11} \frac{\partial^4 w_b}{\partial x^4} - F_{11} \frac{\partial^4 w_s}{\partial x^4} + B_{12} \frac{\partial^3 v}{\partial x^2 \partial y} - E_{12} \frac{\partial^4 w_b}{\partial x^2 \partial y^2} - F_{12} \frac{\partial^4 w_s}{\partial x^2 \partial y^2} + E''_{13} \frac{\partial^2 w_z}{\partial x^2} \\
 & + 2 \frac{\partial B_{11}}{\partial x} \frac{\partial^2 u}{\partial x^2} - 2 \frac{\partial E_{11}}{\partial x} \frac{\partial^3 w_b}{\partial x^3} - 2 \frac{\partial F_{11}}{\partial x} \frac{\partial^3 w_s}{\partial x^3} + 2 \frac{\partial B_{12}}{\partial x} \frac{\partial^2 v}{\partial x \partial y} - 2 \frac{\partial E_{12}}{\partial x} \frac{\partial^3 w_b}{\partial x \partial y^2} \\
 & - 2 \frac{\partial F_{12}}{\partial x} \frac{\partial^3 w_s}{\partial x \partial y^2} + 2 \frac{\partial E''_{13}}{\partial x} \frac{\partial w_z}{\partial x} + \frac{\partial^2 B_{11}}{\partial x^2} \frac{\partial u}{\partial x} - \frac{\partial^2 E_{11}}{\partial x^2} \frac{\partial^2 w_b}{\partial x^2} - \frac{\partial^2 F_{11}}{\partial x^2} \frac{\partial^2 w_s}{\partial x^2} + \frac{\partial^2 B_{12}}{\partial x^2} \frac{\partial v}{\partial y} \\
 & - \frac{\partial^2 E_{12}}{\partial x^2} \frac{\partial^2 w_b}{\partial y^2} - \frac{\partial^2 F_{12}}{\partial x^2} \frac{\partial^2 w_s}{\partial y^2} + \frac{\partial^2 E''_{13}}{\partial x^2} w_z + B_{12} \frac{\partial^3 u}{\partial x \partial y^2} - E_{12} \frac{\partial^4 w_b}{\partial x^2 \partial y^2} - F_{12} \frac{\partial^4 w_s}{\partial x^2 \partial y^2} + B_{22} \frac{\partial^3 v}{\partial y^3} \\
 & - E_{22} \frac{\partial^4 w_b}{\partial y^4} - F_{22} \frac{\partial^4 w_s}{\partial y^4} + E''_{23} \frac{\partial^2 w_z}{\partial y^2} + 2B_{66} \frac{\partial^3 u}{\partial x \partial y^2} + 2B_{66} \frac{\partial^3 v}{\partial x^2 \partial y} - 4E_{66} \frac{\partial^4 w_b}{\partial x^2 \partial y^2} - 4F_{66} \frac{\partial^4 w_s}{\partial x^2 \partial y^2} \\
 & + 2 \frac{\partial B_{66}}{\partial x} \frac{\partial^2 u}{\partial y^2} + 2 \frac{\partial B_{66}}{\partial x} \frac{\partial^2 v}{\partial x \partial y} - 4 \frac{\partial E_{66}}{\partial x} \frac{\partial^3 w_b}{\partial x \partial y^2} - 4 \frac{\partial F_{66}}{\partial x} \frac{\partial^3 w_s}{\partial x \partial y^2} \\
 & = (1 - \mu^2 \nabla^2) \left( I_1 \frac{\partial \ddot{u}}{\partial x} + I_1 \frac{\partial \ddot{v}}{\partial y} + I_0 \ddot{w}_b + I_0 \ddot{w}_s + I_6 \ddot{w}_z - I_2 \frac{\partial^2 \ddot{w}_b}{\partial x^2} - I_4 \frac{\partial^2 \ddot{w}_s}{\partial x^2} - I_2 \frac{\partial^2 \ddot{w}_b}{\partial y^2} - I_4 \frac{\partial^2 \ddot{w}_s}{\partial y^2} + q_3 \right)
 \end{aligned} \tag{12c}$$

**Table 1** Natural frequency of the functionally-graded plates for several FG index

Theory	$k = 0$		$k = 1$			$\frac{a}{h} = 5$		
	$\frac{a}{h} = \sqrt{10}$	$\frac{a}{h} = 10$	$\frac{a}{h} = 5$	$\frac{a}{h} = 10$	$\frac{a}{h} = 20$	$k = 2$	$k = 3$	$k = 5$
3D [36]	0.4658	0.0578	0.2192	0.0596	0.0153	0.2197	0.2211	0.2225
Quasi-3D [38]	–	–	0.2193	0.0596	0.0153	0.2198	0.2212	0.2225
Quasi-3D [37]	–	–	0.2193	0.0596	0.0153	0.2201	0.2216	0.223
Quasi-3D [39]	–	–	0.2193	–	–	0.22	0.2215	0.223
IRPT [40]	0.4661	0.0578	0.2192	0.0597	0.0153	0.2201	0.2214	0.2225
Present	0.4658	0.0578	0.21932	0.0596	0.0153	0.2197	0.2211	0.2225

**Table 2** The efficacy of the nonlocality on the natural frequency of the homogeneous nanoplate

Nonlocality index (nm)	$\frac{h}{a} = 1$			$\frac{h}{a} = 2$		
	Ref ([41])	Ref [42]	Present	Ref ([41])	Ref [42]	Present
0	0.057	0.054	0.057	0.036	0.034	0.036
0.2	0.043	0.040	0.042	0.029	0.028	0.029
0.4	0.028	0.026	0.028	0.021	0.020	0.021
0.6	0.020	0.018	0.020	0.015	0.014	0.015
0.8	0.015	0.014	0.015	0.012	0.011	0.012
1	0.012	0.011	0.012	0.010	0.009	0.010

**Table 3** The efficacy of the nonlocality and geometrical parameters on the natural frequency of the nanoplate ( $T_i = C_i = 0, n_i = m_i = 0$ )

Nonlocality index (nm)	$\frac{b}{a} = 1$		$\frac{b}{a} = 2$		$\frac{b}{a} = 3$	
	$\frac{a}{h} = 5$	$\frac{a}{h} = 10$	$\frac{a}{h} = 5$	$\frac{a}{h} = 10$	$\frac{a}{h} = 5$	$\frac{a}{h} = 10$
0	0.2113	0.0577	0.1377	0.0365	0.1234	0.0325
0.1	0.1931	0.0527	0.1299	0.0345	0.1171	0.0309
0.2	0.1579	0.0431	0.1126	0.0299	0.1029	0.0271
0.3	0.1268	0.0346	0.0948	0.0251	0.0875	0.0231
0.4	0.1036	0.0283	0.0798	0.0212	0.0743	0.0196
0.5	0.0867	0.0237	0.0681	0.0181	0.0638	0.0168
0.6	0.0742	0.0203	0.059	0.0157	0.0555	0.0146
0.7	0.0647	0.0177	0.0519	0.0138	0.0489	0.0129
0.8	0.0572	0.0156	0.0461	0.0122	0.0436	0.0115
0.9	0.0513	0.0140	0.0415	0.011	0.0392	0.0104
1	0.0464	0.0127	0.0377	0.010	0.0357	0.0094

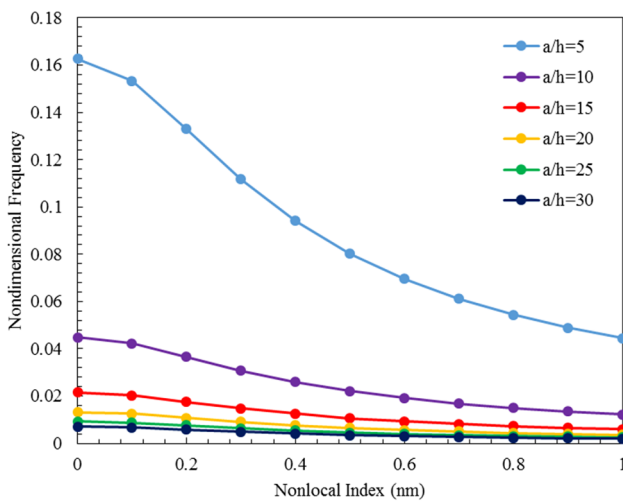


**Fig. 3** The efficacy of the nonlocality and  $\frac{a}{h}$  ratio on the natural frequency of the nanoplate ( $T_i = C_i = 0, n_i = m_i = 0$ )

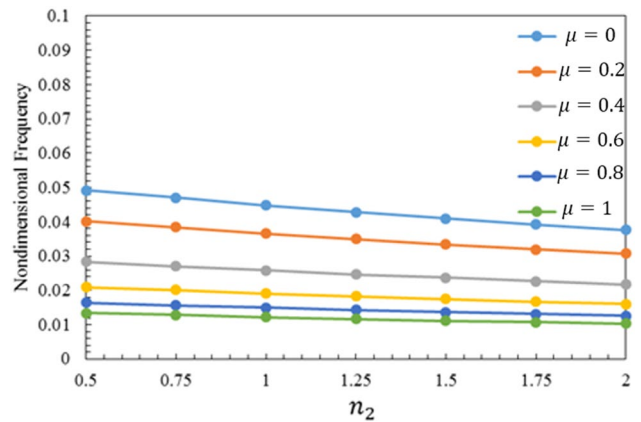


**Fig. 5** The efficacy of the FG parameter on the natural frequency of the nanoplate for several small size impact ( $T_i = C_i = 0, n_2 = m_2, n_1 = m_1 = n_3 = m_3 = 1$ )

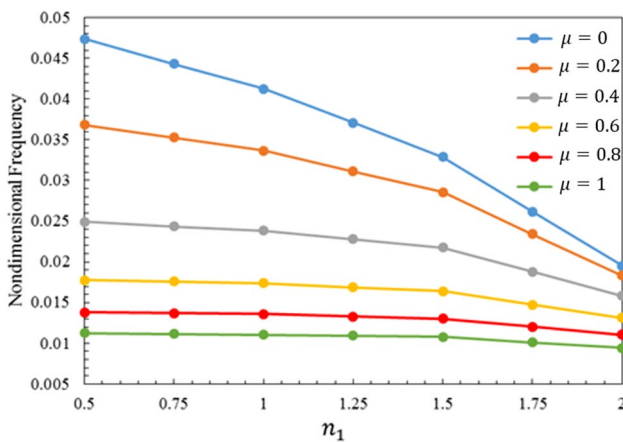


**Fig. 4** The efficacy of the FG parameter on the natural frequency of the nanoplate for several small size impact ( $T_i = C_i = 0, n_i = m_i, n_2 = m_2 = 1$ )

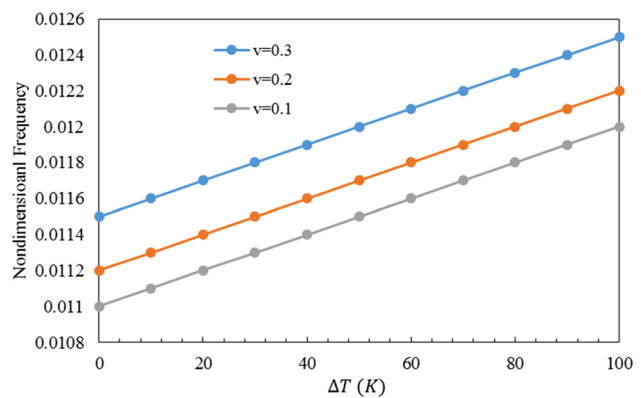


**Fig. 6** The efficacy of the thermal conditions on the frequency of the nanoplate for several Passion's ratio ( $T_2 = T_3 = C_2 = 0, \mu = 1, n_i = m_i = 0 (i = 1, 2, \dots, 4)$ )



$$\begin{aligned}
 & D_{11} \frac{\partial^3 u}{\partial x^3} - F_{11} \frac{\partial^4 w_b}{\partial x^4} - H_{11} \frac{\partial^4 w_s}{\partial x^4} + D_{12} \frac{\partial^3 v}{\partial x^2 \partial y} - F_{12} \frac{\partial^4 w_b}{\partial x^2 \partial y^2} - H_{12} \frac{\partial^4 w_s}{\partial x^2 \partial y^2} + E_{13}''' \frac{\partial^2 w_z}{\partial x^2} \\
 & + 2 \frac{\partial D_{11}}{\partial x} \frac{\partial^2 u}{\partial x^2} - 2 \frac{\partial F_{11}}{\partial x} \frac{\partial^3 w_b}{\partial x^3} - 2 \frac{\partial H_{11}}{\partial x} \frac{\partial^3 w_s}{\partial x^3} + 2 \frac{\partial D_{12}}{\partial x} \frac{\partial^2 v}{\partial x \partial y} - 2 \frac{\partial F_{12}}{\partial x} \frac{\partial^3 w_b}{\partial x \partial y^2} \\
 & - 2 \frac{\partial H_{12}}{\partial x} \frac{\partial^3 w_s}{\partial x \partial y^2} + 2 \frac{\partial E_{13}'''}{\partial x} \frac{\partial w_z}{\partial x} + \frac{\partial^2 D_{11}}{\partial x^2} \frac{\partial u}{\partial x} - \frac{\partial^2 F_{11}}{\partial x^2} \frac{\partial^2 w_b}{\partial x^2} - \frac{\partial^2 H_{11}}{\partial x^2} \frac{\partial^2 w_s}{\partial x^2} + \frac{\partial^2 D_{12}}{\partial x^2} \frac{\partial v}{\partial y} \\
 & - \frac{\partial^2 F_{12}}{\partial x^2} \frac{\partial^2 w_b}{\partial y^2} - \frac{\partial^2 H_{12}}{\partial x^2} \frac{\partial^2 w_s}{\partial y^2} + \frac{\partial^2 E_{13}'''}{\partial x^2} w_z + D_{12} \frac{\partial^3 u}{\partial x \partial y^2} - F_{12} \frac{\partial^4 w_b}{\partial x^2 \partial y^2} - H_{12} \frac{\partial^4 w_s}{\partial x^2 \partial y^2} \\
 & + D_{22} \frac{\partial^3 v}{\partial y^3} - F_{22} \frac{\partial^4 w_b}{\partial y^4} - H_{22} \frac{\partial^4 w_s}{\partial y^4} + E_{23}''' \frac{\partial^2 w_z}{\partial y^2} + 2D_{66} \frac{\partial^3 u}{\partial x \partial y^2} + 2D_{66} \frac{\partial^3 v}{\partial x^2 \partial y} - 4F_{66} \frac{\partial^4 w_b}{\partial x^2 \partial y^2} \\
 & - 4H_{66} \frac{\partial^4 w_s}{\partial x^2 \partial y^2} + 2 \frac{\partial D_{66}}{\partial x} \frac{\partial^2 u}{\partial y^2} + 2 \frac{\partial D_{66}}{\partial x} \frac{\partial^2 v}{\partial x \partial y} - 4 \frac{\partial F_{66}}{\partial x} \frac{\partial^3 w_b}{\partial x \partial y^2} - 4 \frac{\partial H_{66}}{\partial x} \frac{\partial^3 w_s}{\partial x \partial y^2} \\
 & + J_{44} \frac{\partial^2 w_s}{\partial x^2} + J_{44} \frac{\partial^2 w_z}{\partial x^2} + \frac{\partial J_{44}}{\partial x} \frac{\partial w_s}{\partial x} + \frac{\partial J_{44}}{\partial x} \frac{\partial w_z}{\partial x} + J_{55} \frac{\partial^2 w_s}{\partial y^2} + J_{55} \frac{\partial^2 w_z}{\partial y^2} \\
 & = (1 - \mu^2 \nabla^2) \left( I_3 \frac{\partial \dot{u}}{\partial x} + I_3 \frac{\partial \dot{v}}{\partial y} + I_0 \ddot{w}_b + I_0 \ddot{w}_s - I_4 \frac{\partial^2 \ddot{w}_b}{\partial x^2} - I_5 \frac{\partial^2 \ddot{w}_s}{\partial x^2} - I_5 \frac{\partial^2 \ddot{w}_s}{\partial y^2} - I_4 \frac{\partial^2 \ddot{w}_b}{\partial y^2} + I_6 \ddot{w}_z + q_4 \right)
 \end{aligned} \tag{12d}$$

$$\begin{aligned}
 & J_{44} \frac{\partial^2 w_s}{\partial x^2} + J_{44} \frac{\partial^2 w_z}{\partial x^2} + \frac{\partial J_{44}}{\partial x} \frac{\partial w_s}{\partial x} + \frac{\partial J_{44}}{\partial x} \frac{\partial w_z}{\partial x} + J_{55} \frac{\partial^2 w_s}{\partial y^2} + J_{55} \frac{\partial^2 w_z}{\partial y^2} \\
 & - E'_{13} \frac{\partial u}{\partial x} + E''_{23} \frac{\partial^2 w_b}{\partial x^2} + E'''_{23} \frac{\partial^2 w_s}{\partial x^2} - E'_{23} \frac{\partial v}{\partial y} + E''_{23} \frac{\partial^2 w_b}{\partial y^2} + E'''_{23} \frac{\partial^2 w_s}{\partial y^2} - w_z E''_{23} \\
 & = (1 - \mu^2 \nabla^2) (I_6 \ddot{w}_s + I_6 \ddot{w}_b + I_7 \ddot{w}_z + q_5).
 \end{aligned} \tag{12e}$$

The unknown coefficients of Eqs. (12a-e) are reported as following:

$$\begin{aligned}
 (A_{ij}, B_{ij}, E_{ij}, D_{ij}, F_{ij}, H_{ij}) &= \int_{-\frac{h}{2}}^{\frac{h}{2}} C_{ij}(1, z, z^2, f, fz, f^2) dz, (i, j = 1, 2, 6) \\
 (E'_{ij}, E''_{ij}, E'''_{ij}, E''_{ij}) &= \int_{-\frac{h}{2}}^{\frac{h}{2}} C_{ij} \left( \frac{dg}{dz}, z \frac{dg}{dz}, f \frac{dg}{dz}, \left( \frac{dg}{dz} \right)^2 \right) dz \\
 J_{ij} &= \int_{-\frac{h}{2}}^{\frac{h}{2}} C_{ij} g^2 dz
 \end{aligned} \tag{13}$$

### 3 Navier solution method

In the current research, the Navier solution procedure is utilized to achieve the vibration characteristics of the 2D-FG nanoplates with simply supported boundary conditions. Therefore, the relations of the boundary conditions are reported as below:

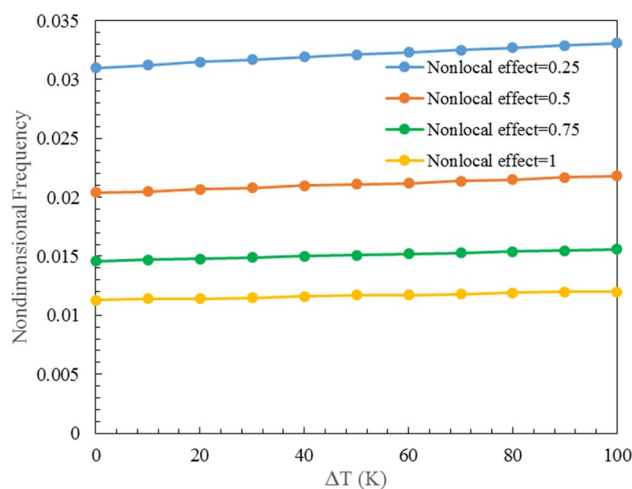
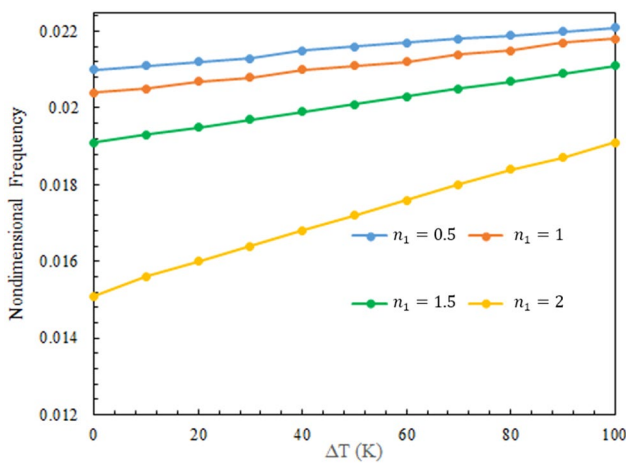


Fig. 7 The variation of the non-dimensional frequency of nano-plate against temperature variation for various nonlocal index ( $n_1 = 1, n_2 = m_2 = 1, T_2 = T_3 = C_1 = 0$ )

**Table 4** The efficacy of the temperature variation and FG parameters on the natural frequency of the FG nanoplate ( $\frac{b}{a} = 1, n_2 = m_2 = 1, T_2 = T_3 = C_1 = 0, \mu = 0.5$ )

$\Delta T(K)$	$n_2 = 1$				$n_2 = 2$			
	$n_1 = 0.5$	$n_1 = 1$	$n_1 = 1.5$	$n_1 = 2$	$n_1 = 0.5$	$n_1 = 1$	$n_1 = 1.5$	$n_1 = 2$
0	0.021	0.0204	0.0191	0.0151	0.0176	0.0168	0.015	0.0083
10	0.0211	0.0205	0.0193	0.0156	0.0177	0.017	0.0153	0.009
20	0.0212	0.0207	0.0195	0.016	0.0178	0.0172	0.0156	0.0098
30	0.0213	0.0208	0.0197	0.0164	0.018	0.0173	0.0158	0.0104
40	0.0215	0.021	0.0199	0.0168	0.0181	0.0175	0.0161	0.0111
50	0.0216	0.0211	0.0201	0.0172	0.0182	0.0177	0.0163	0.0117
60	0.0217	0.0212	0.0203	0.0176	0.0184	0.0178	0.0166	0.0122
70	0.0218	0.0214	0.0205	0.018	0.0185	0.018	0.0168	0.0128
80	0.0219	0.0215	0.0207	0.0184	0.0186	0.0182	0.017	0.0133
90	0.022	0.0217	0.0209	0.0187	0.0188	0.0183	0.0173	0.0138
100	0.0221	0.0218	0.0211	0.0191	0.0189	0.0185	0.0175	0.0143



**Fig. 8** The variation of the non-dimensional frequency of nanoplate against temperature variation for various values of  $n_1$  parameter ( $\frac{b}{a} = 1, n_2 = m_2 = 1, T_2 = T_3 = C_1 = 0, \mu = 0.5$ )

$$\begin{aligned}
 u(x, 0) &= u(x, b) = v(0, y) = v(a, y) = 0 \\
 w_b(x, 0) &= w_b(x, b) = w_b(0, y) = w_b(a, y) = 0 \\
 w_s(x, 0) &= w_s(x, b) = w_s(0, y) = w_s(a, y) = 0 \\
 w_z(x, 0) &= w_z(x, b) = w_z(0, y) = w_z(a, y) = 0
 \end{aligned}
 \tag{14}$$

According to Navier solution procedure, the components of the displacement using double Fourier series are:

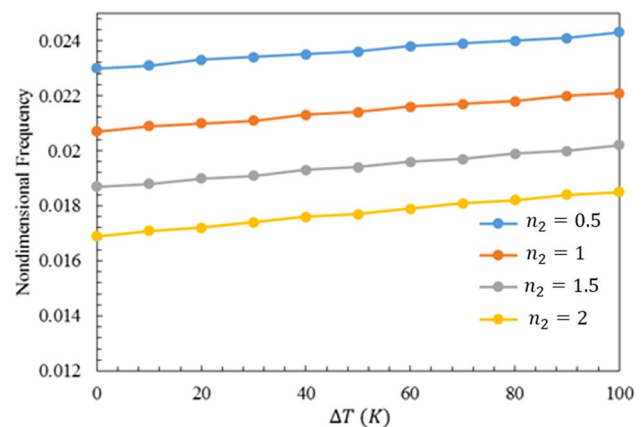


**Fig. 9** The variation of the non-dimensional frequency of nanoplate against temperature variation for various values of  $n_2$  parameter ( $\frac{b}{a} = 1, n_2 = m_2 = 1, T_2 = T_3 = C_1 = 0, \mu = 0.5$ )

$$\begin{aligned}
 u(x, y; t) &= \sum_{r=1}^{\infty} \sum_{s=1}^{\infty} U_{rs} \cos(\alpha x)_r \sin(\beta y)_s e^{i\omega t} \\
 v(x, y; t) &= \sum_{r=1}^{\infty} \sum_{s=1}^{\infty} V_{rs} \sin(\alpha x)_r \cos(\beta y)_s e^{i\omega t} \\
 w_b(x, y; t) &= \sum_{r=1}^{\infty} \sum_{s=1}^{\infty} W_{rs}^b \sin(\alpha x)_r \sin(\beta y)_s e^{i\omega t} \\
 w_s(x, y; t) &= \sum_{r=1}^{\infty} \sum_{s=1}^{\infty} W_{rs}^s \sin(\alpha x)_r \sin(\beta y)_s e^{i\omega t} \\
 w_z(x, y; t) &= \sum_{r=1}^{\infty} \sum_{s=1}^{\infty} W_{rs}^z \sin(\alpha x)_r \sin(\beta y)_s e^{i\omega t}.
 \end{aligned}
 \tag{15}$$

In which  $\omega$  is the frequency of the nanoplate;  $U_{rs}, V_{rs}, W_{rs}^b, W_{rs}^s$  and  $W_{rs}^z$  are the unknown factors,  $\alpha = \frac{r\pi}{a}, \beta = \frac{s\pi}{b}$ . To report the equations of motion in terms of ingredients of displacement, it is essential to substitute Eq. (15) into Eqs. (12a-e) as below:

$$[M_{ij}] \begin{Bmatrix} \ddot{U}_{rs} \\ \ddot{V}_{rs} \\ \ddot{W}_{rs}^b \\ \ddot{W}_{rs}^s \\ \ddot{W}_{rs}^z \end{Bmatrix} + [K_{ij}] \begin{Bmatrix} U_{rs} \\ V_{rs} \\ W_{rs}^b \\ W_{rs}^s \\ W_{rs}^z \end{Bmatrix} = \begin{Bmatrix} 0 \\ 0 \\ Q_{rs} \\ 0 \\ 0 \end{Bmatrix} \tag{16}$$

$$\Rightarrow ([K_{ij}] - \omega^2 [M_{ij}]) \{\Delta\} = 0 \Rightarrow \det([K_{ij}] - \omega^2 [M_{ij}]) = 0 \Rightarrow \omega = (\text{eig}([M]^{-1}[K]))^{0.5}.$$

### 4 Numerical results

In the current research, the vibration investigation of the 2D-FG nanoplates pondering nonlocality subjected to hygrothermo conditions according to a novel HSDT is examined for the first time. The dimensionless forms of the natural frequency parameters are presented as:

$$\begin{aligned} \varpi &= \omega h \sqrt{\frac{\rho}{E}} \\ \varpi &= \frac{\omega a^2}{h} \sqrt{\frac{\rho_m}{E_m}} \end{aligned} \tag{17}$$

The material features of the 2D-FG nanoplate are reported as  $E_m = 70 \text{ GPa}, E_c = 200 \text{ GPa}, \nu_m = \nu_c = 0.34, \rho_m = 2702 \frac{\text{kg}}{\text{m}^3}$  and  $\rho_c = 5700 \frac{\text{kg}}{\text{m}^3}$ .

#### 4.1 Verification of the results

To investigate the accuracy of the current research, first, the outcomes are verified. To verify the outcomes accurately, it is assumed that the material features of the plate vary based on Voigt’s rule of mixtures as following:

$$\begin{aligned} E(z) &= (E_c - E_m) \left(\frac{z}{h} + 0.5\right)^k + E_m \\ \rho(z) &= (\rho_c - \rho_m) \left(\frac{z}{h} + 0.5\right)^k + \rho_m \end{aligned} \tag{18}$$

where  $k$  is the FG index.

In Table 1, the natural frequency of the FG plate for various values of the FG index and  $\frac{a}{h}$ (side-to-thickness) ratio with assumption  $\Delta T = 0, \Delta C = 0, \mu = 0$  has been examined. The results of Refs [36–40] are dedicated to investigate the accuracy of the current model. With investigating the outcomes in Table 1, it can be deduced that the achieving data of the current research are in perfect agreement with similar researches.

In Table 2, the natural frequency of the homogeneous nanoplate for various values of the nonlocality index and  $\frac{b}{a}$  (length -to-side) ratio with assumption  $\Delta T = 0, \Delta C = 0$  has been examined. The results of Refs [41, 42] are dedicated to investigate the accuracy of the current model. With inves-

tigating the outcomes in Table 2, it can be deduced that the achieving data of the current research are in perfect agreement with the similar researches.

#### 4.2 Effects of the nonlocality on the frequency of the nanoplate

In Table 3, the efficacies of the geometrical parameters and nonlocality index are reported on the vibration characteristics of the nanoplates. The results are provided for both thick ( $\frac{a}{h} = 5$ ) and moderately thick ( $\frac{a}{h} = 10$ ) nanoplate. We can declare that the frequency of the nanoplate reduces with growth in  $\frac{a}{h}$  and  $\frac{b}{a}$  ratios. In addition, we can report that with enhancing the value of the nonlocality index, the frequency of the structure reduces. Also, with enhancing the small size parameter, its efficacy on the frequency of the nanosize structure will reduce. Also, we can report that with increasing the small size parameter, the efficacy of the thickness stretching on the frequency of the nanoplate reduces. Therefore, we can render that with enhancing the stiffness of the structure (i.e., with reducing the nonlocality index), the thickness stretching has essential impacts on the responses of the nanosize systems.

In Fig. 3, the efficacies of the nonlocality index and  $\frac{a}{h}$  ratio on the vibration characteristics of the nanoplate are examined. The results are provided for thick ( $\frac{a}{h} = 5$ ), moderately thick ( $\frac{a}{h} = 10$ ) and thin ( $\frac{a}{h} = 30$ ) nanoplates. We can declare that the natural frequency of the nanoplate reduces with growth in  $\frac{a}{h}$  ratio. Also, we can report that with enhancing/reducing the side/thickness of the nanoplate, its efficacy on the frequency of the nanoplate will reduce. Moreover, with enhancing the nonlocality index, the efficacy of the thickness stretching on the frequency of the nanoplate reduces. Also, in thick nanoplates ( $\frac{a}{h} = 5$ ), nonlocality index has essential role on the mechanical responses of the system. However, in thin nanoplates ( $\frac{a}{h} = 30$ ), nonlocality index has minor role on the mechanical responses of the system. Therefore, it is

noticeable that in thin nanoplates, the efficacy of the nonlocality is neglectable.

In Fig. 4, the efficacies of the nonlocality index and FG parameters on the frequency of the nanoplate are reported. We can declare that with enhancing the value of  $n_1$ , the frequency of the nanoplate decreases. This is because with enhancing the FG index, the value of the components of the mass matrix of the system increase. Also, with reducing/increasing the value of  $n_1$ , its efficacy on the frequency of the nanoplate reduces/enhances. Also, with enhancing/reducing the value of  $n_1$ , the efficacy of the nonlocality index on the frequency of the nanoplate reduces/enhances. Moreover, when we ponder the nonlocality, FG indexes have important role on the dynamic responses of the FG nanoplate.

In Fig. 5, the efficacies of the size effect parameter and FG indexes on the frequency of the nanoplate are reported. We can declare that with enhancing the value of  $n_2$ , the frequency of the nanoplate reduces. This is because with enhancing the FG indexes, the value of the components of the mass matrix of the system increase. Also, with increasing/reducing the nonlocality index, its efficacy on the vibration characteristics of the nanoplate will reduce/enhance.

### 4.3 Effects of the hygro-thermo conditions on the frequency of the nanoplate

In this part, the natural frequency investigation of the 2D-FG nanoplates in the hygro-thermo conditions is reported.

In Fig. 6, the variation of the non-dimensional frequency of the 2D-FG nanoplate against temperature variation for various Passion's ratio is presented. We can express that with increasing the Passion's ratio, the natural frequency of the 2D-FG nanoplate enhances. Also, with increasing the temperature variation, the natural frequency of the 2D-FG nanoplate rises linearly. In addition, with enhancing the temperature variation, the frequency chart behaves similarly for various values of Passion's ratio.

In Fig. 7, the variation of the non-dimensional frequency of the 2D-FG nanoplate against temperature variation for various nonlocal size effect is presented. We can express that with increasing the nonlocal size effect, the natural frequency of the 2D-FG nanoplate decreases. Also, with increasing the temperature variation, the natural frequency of the 2D-FG nanoplate increases linearly. In addition, with enhancing the size effect parameter, its impact on the natural frequency of the plate reduces. Moreover, with enhancing/reducing the nonlocality index, the impacts of the temperature variation on the natural frequency of the 2D-FG nanoplate will reduce/increase. Therefore, we can conclude that with increasing the size effect parameter, the slope of the chart will reduce when the variation of the temperature rises.

In Table 4, the variation of the non-dimensional frequency of the 2D-FG nanoplate against temperature variation for various FG parameters is presented. We can express that with increasing the temperature variation, the natural frequency of the 2D-FG nanoplate increases. Also, with increasing the FG parameters ( $n_1, n_2$ ), the natural frequency of the nanoplate decreases. This is because when the FG parameters increase, the stiffness of the system increases, however; the components of the mass matrix of the system increase more than components of the stiffness matrix (For more detail, please refer to Eqs. (12a–e)). Therefore, with increasing the FG parameters, the natural frequency of the nanoplate will decrease. In addition, with increasing the value of  $n_1$  parameter, its impact on the natural frequency of the 2D-FG nanoplate will increase when the temperature variation grows. Also, with increasing the values of  $n_2$  parameter, its effects on the natural frequency of the 2D-FG nanoplate will enhance when the temperature variation increases.

In Fig. 8, the variation of the non-dimensional frequency of the 2D-FG nanoplate against temperature variation for several values of  $n_1$  parameter is presented. We can express that with increasing/decreasing the temperature variation, the impacts of the  $n_1$  parameter on the frequency of the plate will decrease/rise. Also, with growing/decreasing the values of the  $n_1$  parameter, the impacts of the temperature variation on the natural frequency of the plate will rise/decrease.

In Fig. 9, the variation of the non-dimensional frequency of the 2D-FG nanoplate against temperature variation for various values of  $n_2$  parameter is presented. We can express that with enhancing the temperature variation, the frequency chart behaves similarly for several values of  $n_2$  parameter. Moreover, with enhancing the temperature variation, the intensity of the increase in frequencies are the same for various values of  $n_2$  parameter.

## 5 Conclusions

In the current research, a novel nonlocal higher-order theory is presented to inquire about the free vibration analysis of the 2D-FG nanoplate subjected to hygro-thermo loading. The novelty of the current research is to present a new HSST, which is an amalgamation of exponential, polynomial and trigonometric functions. Thickness stretching influence is considered according to higher-order shear and normal deformation theory. Size-dependent nonlocal elasticity theory is dedicated to pondering the nonlocality. The transverse component of displacement is divided into bending and shear components. To ponder the effects of the thermal and moisture conditions on the vibration characteristics of

the 2D-FG nanoplate, we ponder the nonlinear relations for temperature and moisture fields. Hamilton's axiom is dedicated to achieving the governing equations of motion. Then, the Navier solution technique is dedicated to derive the natural frequency of the nanoplate with S–S boundary conditions. The achieved results of the current research are:

- The frequency of the nanoplate reduces with growth in  $\frac{a}{h}$  and  $\frac{b}{a}$  ratios.
- With enhancing the value of the nonlocality index, the frequency of the structure reduces.
- With enhancing the nonlocality index, its efficacy on the frequency of the nanosize structure will reduce.
- In thick nanoplates, nonlocality index has vital role in the mechanical responses of the nanoplates. However, in thin nanoplates, nonlocality index has a minor role in the mechanical responses of the nanoplates.
- With enhancing the value of FG indexes, the frequency of the nanoplate decreases.
- With increasing/decreasing the size effect parameter, the impacts of the temperature variation on the natural frequency of the 2D-FG nanoplate will reduce/increase.
- With increasing/decreasing the temperature variation, the impacts of the  $n_1$  parameter on the frequency of the plate will decrease/increase.
- With enhancing the temperature variation, the frequency chart behaves similarly for various values of  $n_2$  parameter.
- With enhancing the temperature variation, the frequency chart increases similarly for various values of Passion's ratio.
- With increasing the values of FG indexes, their impacts on the natural frequency of the 2D-FG nanoplate will increase when the temperature variation rises.

**Acknowledgements** This research is financially supported by the Natural Science Foundation of Zhejiang province, China (No. LY20A020005), preparatory funds of School of Architecture and Transportation, Ningbo university of technology, Open Research Fund Program of State key Laboratory of Hydrosience and Engineering.

## References

1. Karami B, Janghorban M, Tounsi A (2019) Galerkin's approach for buckling analysis of functionally graded anisotropic nanoplates/different boundary conditions. *Eng Comput* 35(4):1297–1316
2. Phung-Van P, Thai CH (2021) A novel size-dependent nonlocal strain gradient isogeometric model for functionally graded carbon nanotube-reinforced composite nanoplates. *Eng Comput*. <https://doi.org/10.1007/s00366-021-01353-3>
3. Sahmani S, Fattahi AM, Ahmed NA (2020) Analytical treatment on the nonlocal strain gradient vibrational response of postbuckled functionally graded porous micro-/nanoplates reinforced with GPL. *Eng Comput* 36(4):1559–1578
4. Wu H, Liu H (2020) Nonlinear thermo-mechanical response of temperature-dependent FG sandwich nanobeams with geometric imperfection. *Eng Comput*. <https://doi.org/10.1007/s00366-020-01005-y>
5. Mallek H, Jrad H, Wali M, Dammak F (2019) Nonlinear dynamic analysis of piezoelectric-bonded FG-CNTR composite structures using an improved FSDT theory. *Eng Comput* 37:1–19
6. Ghayesh MH (2019) Viscoelastic mechanics of Timoshenko functionally graded imperfect microbeams. *Compos Struct* 225:110974
7. Ghayesh MH (2018) Nonlinear vibration analysis of axially functionally graded shear-deformable tapered beams. *Appl Math Model* 59:583–596
8. Zenkour AM (2020) Quasi-3D Refined Theory for Functionally Graded Porous Plates: Displacements and Stresses. *Phys Mesomech* 23(1):39–53
9. Jalaei MH, Thai HT (2019) Dynamic stability of viscoelastic porous FG nanoplate under longitudinal magnetic field via a nonlocal strain gradient quasi-3D theory. *Compos Part B Eng* 175:107164
10. Mirjavadi SS, Afshari BM, Barati MR, Hamouda AMS (2019) Transient response of porous FG nanoplates subjected to various pulse loads based on nonlocal stress-strain gradient theory. *Eur J Mech-A/Solids* 74:210–220
11. Sahmani S, Safaei B (2019) Nonlocal strain gradient nonlinear resonance of bi-directional functionally graded composite micro/nano-beams under periodic soft excitation. *Thin-Walled Struct* 143:106226
12. Cao Y, Khorami M, Baharom S, Assilzadeh H, Dindarloo MH (2021) The effects of multi-directional functionally graded materials on the natural frequency of the doubly-curved nanoshells. *Compos Struct* 258:113403
13. Kazemirad S, Ghayesh MH, Amabili M (2013) Thermo-mechanical nonlinear dynamics of a buckled axially moving beam. *Arch Appl Mech* 83(1):25–42
14. Ghayesh MH, Kazemirad S, Darabi MA, Woo P (2012) Thermo-mechanical nonlinear vibration analysis of a spring-mass-beam system. *Arch Appl Mech* 82(3):317–331
15. Ghayesh MH, Amabili M, Païdoussis MP (2012) Thermo-mechanical phase-shift determination in Coriolis mass-flowmeters with added masses. *J Fluids Struct* 34:1–13
16. Ghayesh MH, Amabili M (2015) Nonlinear stability and bifurcations of an axially moving beam in thermal environment. *J Vib Control* 21(15):2981–2994
17. Daikh AA, Draï A, Bensaid I, Houari MSA, Tounsi A (2020) On vibration of functionally graded sandwich nanoplates in the thermal environment. *J Sandw Struct Mater*. <https://doi.org/10.1177/1099636220909790>
18. Hosseini M, Jamalpoor A, Bahreman M (2016) Small-scale effects on the free vibrational behavior of embedded viscoelastic double-nanoplate-systems under thermal environment. *Acta Astronaut* 129:400–409
19. Daikh AA, Bachiri A, Houari MSA, Tounsi A (2020) Size dependent free vibration and buckling of multilayered carbon nanotubes reinforced composite nanoplates in thermal environment. *Mech Based Des Struct Mach*. <https://doi.org/10.1080/15397734.2020.1752232>
20. Singh PP, Azam MS (2020) Free vibration and buckling analysis of elastically supported transversely inhomogeneous functionally graded nanoplate in thermal environment using Rayleigh–Ritz method. *J Vib Control*. <https://doi.org/10.1177/1077546320966932>
21. Dastjerdi S, Malikan M, Dimitri R, Tornabene F (2021) Nonlocal elasticity analysis of moderately thick porous functionally graded plates in a hygro-thermal environment. *Compos Struct* 255:112925

22. Chen T, Chen H, Liu L (2020) Vibration energy flow analysis of periodic nanoplate structures under thermal load using fourth-order strain gradient theory. *Acta Mech* 231(10):4365–4379
23. Fang J, Zheng S, Xiao J, Zhang X (2020) Vibration and thermal buckling analysis of rotating nonlocal functionally graded nanobeams in thermal environment. *Aerosp Sci Technol* 106:106146
24. Kolahdouzan F, Mosayyebi M, Ghasemi FA, Kolahchi R, Panah SRM (2020) Free vibration and buckling analysis of elastically restrained FG-CNTRC sandwich annular nanoplates. *Adv Nano Res* 9(4):237–250
25. Dindarloo MH, Zenkour AM (2020) Nonlocal strain gradient shell theory for bending analysis of FG spherical nanoshells in thermal environment. *Eur Phys J Plus* 135(10):1–18
26. Mashat DS, Zenkour AM, Radwan AF (2020) A quasi 3-D higher-order plate theory for bending of FG plates resting on elastic foundations under hygro-thermo-mechanical loads with porosity. *Eur J Mech-A/Solids* 82:103985
27. Lal R, Saini R (2020) Vibration analysis of functionally graded circular plates of variable thickness under thermal environment by generalized differential quadrature method. *J Vib Control* 26(1–2):73–87
28. Thang PT, Tran P, Nguyen-Thoi T (2021) Applying nonlocal strain gradient theory to size-dependent analysis of functionally graded carbon nanotube-reinforced composite nanoplates. *Appl Math Model* 93:775–791
29. Arshid E, Arshid H, Amir S, Mousavi SB (2021) Free vibration and buckling analyses of FG porous sandwich curved microbeams in thermal environment under magnetic field based on modified couple stress theory. *Arch Civ Mech Eng* 21(1):1–23
30. Esen I, Özarpa C, Eltahir MA (2021) Free vibration of a cracked FG microbeam embedded in an elastic matrix and exposed to magnetic field in a thermal environment. *Compos Struct* 261:113552
31. Thai HT, Choi DH (2014) Improved refined plate theory accounting for effect of thickness stretching in functionally graded plates. *Compos B Eng* 56:705–716
32. Karama M, Afaq KS, Mistou S (2009) A new theory for laminated composite plates. *Proc Inst Mech Eng Part L J Mater Des Appl* 223:53–62
33. Reddy JN (1984) A simple higher-order theory for laminated composite plates. *J Appl Mech* 51:745
34. Soldatos KP (1992) A transverse shear deformation theory for homogeneous monoclinic plates. *Acta Mech* 94:195–220
35. Thai CH, Kulasegaram S, Tran LV, Nguyen-Xuan H (2014) Generalized shear deformation theory for functionally graded isotropic and sandwich plates based on isogeometric approach. *Comput Struct* 141:94–112
36. Vel SS, Batra RC (2004) Three-dimensional exact solution for the vibration of functionally graded rectangular plates. *J Sound Vib* 272(3–5):703–730
37. Neves AMA, Ferreira AJM, Carrera E, Cinefra M, Roque CMC, Jorge RMN et al (2012) A quasi-3D hyperbolic shear deformation theory for the static and free vibration analysis of functionally graded plates. *Compos Struct* 94(5):1814–1825
38. Neves AMA, Ferreira AJM, Carrera E, Roque CMC, Cinefra M, Jorge RMN et al (2012) A quasi-3D sinusoidal shear deformation theory for the static and free vibration analysis of functionally graded plates. *Compos Part B Eng* 43(2):711–725
39. Neves AMA, Ferreira AJM, Carrera E, Cinefra M, Roque CMC, Jorge RMN et al (2013) Static, free vibration and buckling analysis of isotropic and sandwich functionally graded plates using a quasi-3D higher-order shear deformation theory and a meshless technique. *Compos Part B Eng* 44(1):657–674
40. Abdelaziz HH, Atmane HA, Mechab I, Boumia L, Tounsi A, Abbas ABE (2011) Static analysis of functionally graded sandwich plates using an efficient and simple refined theory. *Chin J Aeronaut* 24(4):434–448
41. Nami M, Janghorban M (2015) Free vibration analysis of rectangular nano-plates based on twovariable refined plate theory using a new strain gradient elasticity theory. *J Braz Soc Mech Sci Eng* 37(1):313–324
42. Dindarloo MH, Li L (2019) Vibration analysis of carbon nanotubes reinforced isotropic doubly curved nanoshells using nonlocal elasticity theory based on a new higher order shear deformation theory. *Compos Part B Eng* 175:107170

**Publisher's Note** Springer Nature remains neutral with regard to jurisdictional claims in published maps and institutional affiliations.